AD-A147 721 ELECTRONIC STRUCTURE CHEMICAL BONDING AND ELECTRON CONDUCTIVITY OF THIN-F..(U) MASSACHUSETTS INST OF TECH CAMBRIDGE DEPT OF MATERIALS SCIENC.. 1/1

UNCLASSIFIED K H JOHNSON ET AL. 10 SEP 84 TR-8 F/G 20/12 NL

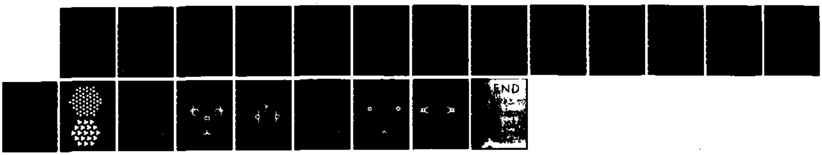

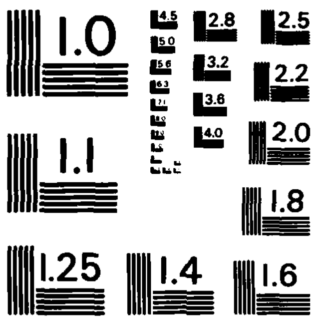

MICROCOPY RESOLUTION TEST CHART
NATIONAL BUREAU OF STANDARDS-1963-A

Unclassified

SECURITY CLASSIFICATION OF THIS PAGE (When Data Entered)

REPORT DOCUMENTATION PAGE

READ INSTRUCTIONS BEFORE COMPLETING FORM

1. REPORT NUMBER: 8	2. GOVT ACCESSION NO.
3. RECIPIENT'S CATALOG NUMBER	
4. TITLE (and Subtitle): Electronic Structure, Chemical Bonding, and Electron Conductivity of Thin-Film Transition-Metal Silicides	5. TYPE OF REPORT & PERIOD COVERED: Interim
	6. PERFORMING ORG. REPORT NUMBER
7. AUTHOR(s): K. H. Johnson and F. A. Leon	8. CONTRACT OR GRANT NUMBER(s): N00014-81-K-0499
9. PERFORMING ORGANIZATION NAME AND ADDRESS: Center for Materials Science and Engineering, M.I.T., Cambridge, Massachusetts 02139	10. PROGRAM ELEMENT, PROJECT, TASK AREA & WORK UNIT NUMBERS: Task No. Nr 056-757
11. CONTROLLING OFFICE NAME AND ADDRESS: Office of Naval Research, Department of the Navy, Arlington, Virginia 22217	12. REPORT DATE: September 10, 1984
	13. NUMBER OF PAGES: 17
14. MONITORING AGENCY NAME & ADDRESS (if different from Controlling Office)	15. SECURITY CLASS. (of this report): Unclassified
	15a. DECLASSIFICATION/DOWNGRADING SCHEDULE

16. DISTRIBUTION STATEMENT (of this Report)

Approval for public release;
distribution unlimited.

17. DISTRIBUTION STATEMENT (of the abstract entered in Block 20, if different from Report)

18. SUPPLEMENTARY NOTES

Prepared for Publication in Solid State Communications

19. KEY WORDS (Continue on reverse side if necessary and identify by block number)

electronic structure
chemical bonding
electron conductivity
thin-film transition-metal silicides

20. ABSTRACT (Continue on reverse side if necessary and identify by block number)

The local electronic densities of states and chemical bonding of thin-film palladium and molybdenum silicides are compared on the basis of embedded cluster molecular-orbital calculations. Composite Pd(d)-Si(p)antibonding/Si(p)-Si(p)bonding character and composite Mo(d)-Si(p)nonbonding/Mo(d)-Si(d)bonding character at the respective Fermi energies are responsible for the different electrical conductivities of these silicide films and for the different Schottky barriers of the corresponding silicide/silicon systems.

DD FORM 1 JAN 73 1473 EDITION OF 1 NOV 65 IS OBSOLETE
S/N 0102-LF-014-6601

Unclassified

SECURITY CLASSIFICATION OF THIS PAGE (When Data Entered)

SECURITY CLASSIFICATION OF THIS PAGE (When Data Entered)

SECURITY CLASSIFICATION OF THIS PAGE(When Data Entered)

OFFICE OF NAVAL RESEARCH

Contract No. N00014-81-K-0499

Task No. Nr 056-757

TECHNICAL REPORT NO. 8

ELECTRONIC STRUCTURE, CHEMICAL BONDING, AND ELECTRON CONDUCTIVITY OF THIN-FILM TRANSITION-METAL SILICIDES

by

K. H. Johnson and F. A. Leon

Department of Materials Science and Engineering
Massachusetts Institute of Technology
Cambridge, Massachusetts 02139

September 10, 1984

ELECTRONIC STRUCTURE, CHEMICAL BONDING, AND ELECTRON CONDUCTIVITY OF THIN-FILM TRANSITION-METAL SILICIDES*

K. H. Johnson and F. A. Leon
Department of Materials Science and Engineering
Massachusetts Institute of Technology
Cambridge, Massachusetts 02139

Abstract

The local electronic densities of states and chemical bonding of thin-film palladium and molybdenum silicides are compared on the basis of embedded cluster molecular-orbital calculations. Composite Pd(d)-Si(p)antibonding/Si(p)-Si(p)bonding character and composite Mo(d)-Si(p)nonbonding/Mo(d)-Si(d)bonding character at the respective Fermi energies are responsible for the different electrical conductivities of these silicide films and for the different Schottky barriers of the corresponding silicide/silicon systems.

---

*Research sponsored by the Office of Naval Research.

Thin-film transition-metal silicides are being used to an increasing extent as interconnect and gate materials in very-large-scale-integrated (VLSI) circuits [1-3]. Experimental [4-6] and theoretical [7-9] studies, focussed primarily on the near-noble Pd, Ni, and Pt/silicon interfaces and silicides, have established the importance of chemical intermixing and bond formation in determining Schottky barrier height and electron transport across transition-metal silicide/silicon interfaces. Such issues are also expected to be of significance in refractory transition-metal (e.g. Mo, W, and Nb) silicide/silicon interfaces, which are of great current technological interest for high-speed VLSI computer circuits [10], but have not been the subjects of much fundamental experimental or theoretical investigation [11].

In this communication, we present quantitative theoretical models for the electronic structures and chemical bonding of thin-film palladium and molybdenum silicides. Because of the importance of local chemical bonding, the electronic structures have been calculated by a "real-space" molecular-orbital approach rather than a "reciprocal-" or "k-space" band-structure method. The approach used is the recently developed iterative partitioned scattered-wave method [12], which permits the computation of molecular orbitals and local densities of states for subclusters of an extended solid or interface, including the effects of "embedding" the subclusters in the extended environment. This method is combined with the Xalpha approximation to electron-electron exchange and correlation [13], which has traditionally been used with the scattered-wave method in its conventional form [14,15]. The standard Xalpha scattered-wave

molecular-orbital method has already been applied successfully to elucidate the local electronic structures of hydrogenated amorphous silicon [16] and crystalline silicon containing substitutional [17,18] and interstitial [19] transition-metal impurities.

In the iterative partitioning version of the scattered-wave technique [12], the secular equation for the molecular orbitals of large silicide aggregates, such as the Pd_2Si monolayer thin films shown in Fig. 1(a) and (b), consisting of the respective encircled $SiPd_3$ and Pd_3Si_6 subclusters and the surrounding extended silicide environment, can be written in the matrix form:

$$\begin{bmatrix} T_a^{-1} & G_{ab} \\ G_{ba} & T_b^{-1} \end{bmatrix} \begin{bmatrix} A_a \\ A_b \end{bmatrix} = 0 \qquad (1)$$

Here T_a represents the electron-wave scattering matrix of the silicide subcluster and T_b represents the scattering matrix of the surrounding environment; G_{ab} and G_{ba} are matrices which represent the "propagation" of electron waves between the silicide subcluster and its environment; and A_a and A_b are the electron wavefunction amplitudes emanating from the silicide subcluster and environment, respectively. To make the solution of Eq. (1) practical, we first contract the matrix of (1) using a simple property of linear algebra [20]. This leads to the matrix equation:

$$(T_a^{-1} - G_{ab}T_bG_{ba})A_a = 0 \qquad (2)$$

for the molecular orbitals of the silicide subcluster, <u>including</u> the effects of coupling to the silicide environment through the terms $G_{ab}T_bG_{ba}$. Solving the contracted secular equation (2) is much more computationally efficient than solving the complete secular equation (1). The following iterative procedure is used to solve Eq. (2): First, an energy eigenvalue E_0 is found from the subcluster submatrix T_a^{-1}, including only the molecular potential field of the surrounding silicide environment. Then the matrix elements of $G_{ab}T_bG_{ba}$ are calculated using E_0 as the trial energy. Finally, determinants of the matrix

$$[T_a(E)]^{-1} - G_{ab}(E_0)T_b(E_0)G_{ba}(E_0) \qquad (3)$$

are calculated at various values of the energy E until a zero is found. This value of E (call it E_1) is assumed to be an approximate solution of (2). If E_1 differs considerably from E_0, the procedure is repeated from the second step using

$$E = cE_0 + (1 - c)E_1 \quad (0 < c < 1) \qquad (4)$$

as the next energy. In the last step of this procedure, the matrix elements of G_{ab}, T_b, and G_{ba} are unchanged, so they must be calculated only once per iteration. Therefore, this procedure leads to a very substantial improvement in computational efficiency over the direct solution of Eq. (1).

The resulting local electronic densities of states for the encircled subclusters of the Pd_2Si monolayers of Fig. 1(a) and (b),

respectively, including the effects of "embedding" the subclusters in the surrounding silicide environment, are shown as the solid and dashed curves, respectively in Fig. 2(a) and (b). Consistent with recent band-structure studies of epitaxial Pd_2Si layers on a Si(111) surface [9], for each monolayer there is a large peak in the density of states between 1 and 3 eV below the Fermi energy E_F. The peak for layer (b) of Fig. 1 occurs at somewhat lower (more negative) energy, relative to the Fermi energy, and is somewhat broader than the peak for layer (a) of Fig. 1. This is due to the bonding interaction among the the Pd(d) orbitals (i. e. "d-band" formation) of the triangular Pd_3 clusters in layer (b). The calculated molecular orbitals corresponding to these peaks are Pd(d) nonbonding with respect to the Si(p) orbitals. The secondary peaks immediately below and above the nonbonding peaks correspond, respectively, to Pd(d)-Si(p) bonding and antibonding molecular orbitals. Indeed, the Fermi level coincides with Pd(d)-Si(p) antibonding states. Within layer (a) of Fig 1, these antibonding states are represented by the $SiPd_3$ subcluster molecular-orbital wavefunction contour map shown in Fig. 3(a). Within layer (b) of Fig. 1, these Pd(d)-Si(p) antibonding states are actually bonding between the Si(p) orbitals; as revealed by the molecular-orbital contour map shown in Fig 3(b). In other words, for a thin Pd_2Si film consisting of composite layers (a) and (b) of the type shown in Fig. 1, the Fermi level is "pinned" by electronic states of composite Pd(d)-Si(p)antibonding/Si(p)-Si(p)bonding character. These states lie near the top of the Si(p)-Si(p) bonding valence band of silicon and are responsible for the relatively large Schottky barrier

observed for the Pd_2Si/Si system [11]. As will be demonstrated below, this composite Pd(d)-Si(p) antibonding/Si(p)-Si(p) bonding character at the Fermi energy also largely determines the electrical conductivity of a Pd_2Si thin film.

The calculated local density of states for an $SiMo_3$ subcluster of an $MoSi_2$ monolayer is shown in Fig. 4. In contrast to the above results for Pd_2Si, the Fermi energy concides with a high density of Mo(d) states which are nonbonding with respect to the Si(p) orbitals. These states lie well above the Si(p)-Si(p) bonding states that correspond to the top of the valence band of silicon. They are responsible for pinning the Fermi level and for the smaller Schottky barrier of the $MoSi_2/Si$ system relative to that of the Pd_2Si/Si system [11]. A close examination of the molecular-orbital topology of these states, as exemplified by the wavefunction contour maps in Fig. 5, reveals that the Mo(d) orbitals, while nonbonding with respect to the Si(p) valence orbitals, are actually weakly bonding with respect to the virtual Si(d) orbitals. Although one usually ignores Si(d) orbitals as being relevant to solid-state electronic structure-properties relations, in this situation these orbitals act as a "pathway" for promoting overlap and metallic bonding among the d orbitals of the Mo atoms which are only second-nearest neighbors in the silicide monolayer. It is also evident from these results (see below) that spatially delocalized Mo(d)-Si(d) bonding of the type shown in Fig. 5 is largely responsible for the electrical conductivity of an $MoSi_2$ thin film.

The computed molecular orbitals can be used as a basis for calculating the electrical conductivities of these thin-film

silicides via Kubo theory [21]. Kubo's formula for the conductivity can be reduced approximately (for "room temperature") to the form [22]

$$\sigma = 2\pi^2 n e^2 d^2/h \qquad (5)$$

where d is the molecular-orbital bond distance at the Fermi energy and n is the bond electron density at the Fermi energy. The Si(p)-Si(p) bond distance in Fig. 3(b) is 3.8A, whereas the Mo(d)-Si(d) bond length in Fig. 5 is 2.6 A. The corresponding values of n, obtained from the computed molecular-orbital components, are 3×10^{22} and 2×10^{22} cm^{-3},respectively. Substitution of these values of d and n in Eq. (5) yields conductivities of 3.3×10^{5} and 1.0×10^{4} $(ohm\text{-}cm)^{-1}$ for the Pd_2Si and $MoSi_2$ layers, respectively, which correspond to resistivities of 30×10^{6} and 97×10^{6} ohm-cm. These values are in good agreement with experiment [1]. Thus the difference in the chemical bonding at the Fermi energies of Pd_2Si and $MoSi_2$ thin films accounts for their respective electrical conductivities.

In conclusion, it has been shown that the detailed composite molecular-orbital topology of the electronic states around the Fermi energy is key to understanding the specific electrical properties of thin-film transition-metal silicides. Such knowledge may possibly be put to use in the development and refinement of silicide/silicon VLSI microstructures.

References

1. D. B. Fraser, in **VLSI Technology**, edited by S. M. Sze (McGraw-Hill, New York, 1983), p. 372.

2. B. L. Crowder and S. Zirinsky, IEEE Trans. Electron Devices **26**, 369 (1979).

3. S. P. Murarka and D. B. Fraser, J. Appl. Phys. **51**, 342 (1980).

4. J. L. Freeouf, G. W. Rubloff, P. S. Ho, and T. S. Kuan, Phys. Rev. Lett. **43**, 1836 (1979); G. W. Rubloff, P. S. Ho, J. F. Freeouf, and J. E. Lewis, Phys. Rev. **B23**, 4183 (1981).

5. P. J. Grunthaner, F. J. Grunthaner, and A. Madhukar, J. Vac. Sci. Technol. **21**, 837 (1982); Physica **117B & 118B**, 831 (1983).

6. G. W. Rubloff, Surf. Sci. **132**, 268 (1983).

7. P. S. Ho, G. W. Rubloff, J. E. Lewis, V. L. Moruzzi, and A. R. Williams, Phys. Rev. **B22**, 4784 (1980).

8. F. Herman, F. Casula, and R. V. Kasowski, in **Proceedings of the 16th International Conference on the Physics of Semiconductors**, Montpelier, France, Sept. 6-10, 1982, Physica B, in press.

9. O. Bisi and K. N. Tu, Phys. Rev. Lett. **352**, 1633 (1984).

10. A. J. Steckl and T. P. Chow, in **Proceedings of the 4th International Brazil Conference on Microelectronics**, Campinas, Brazil, February 22, 1983, in press.

11. L. J. Brillson, Surface Sci. Repts. **2**, 123 (1982).

12. F. A. Leon, Ph.D. Thesis, Department of Physics, Massachusetts Institute of Technology, February, 1984; F. A. Leon and K. H. Johnson, Chem. Phys. Lett., in press.

13. J. C. Slater and K. H. Johnson, Phys. Rev. **B5**, 844 (1972).

14. K. H. Johnson, in **Advances in Quantum Chemistry**, Vol 7, edited by P. -O. Lowdin (Academic, New York, 1973), p. 143.

15. J. W. D. Connolly, in **Modern Theoretical Chemistry**, Vol 7, edited by G. A. Segal (Plenum, New York, 1977), p. 105.

16. K. H. Johnson, H. J. Kolari, J. P. deNeufville, and D. L. Morel, Phys. Rev. **B21**, 643 (1980); M. E. Eberhart, K. H. Johnson, and D. Adler, Phys. Rev. **B26**, 3138 (1982).

17. B. G. Cartling, J. Phys. **C8**, 3171, 3183 (1975)

18. L. A. Hemstreet, Phys. Rev. **B15**, 834 (1977).

19. G. G. DeLeo, G. D. Watkins, and W. B. Fowler, Phys. Rev. **B23**, 1851 (1981); **B25**, 4962, 4972 (1982); G. D. Watkins, G. G. DeLeo, and W. B. Fowler, Physica **116B**, 28 (1983).

20. P. -O. Lowdin, J. Mol. Spectry. **14**, 112 (1964).

21. R. Kubo, J. Phys. Soc. Japan **12**, 570 (1957).

22. K. H. Johnson, to be published.

Figure Captions

Fig. 1. Monolayer structures of Pd_2Si. Solid circles represent Pd atoms; open circles represent Si atoms. The principal subclusters defined in the partitioned scattered-wave molecular-orbital calculations are encircled (dashed circles).

Fig. 2. Subcluster local electronic densities of states for Pd_2Si monolayers (a) (solid profile) and (b) (dashed profile) of Fig. 1, as computed by the partitioned scattered-wave method. The principal chemical bonding, nonbonding, and antibonding characters of the component molecular orbitals are indicated.

Fig. 3. (a) Contour map of the Pd(d)-Si(p) antibonding molecular-orbital wavefunction at the Fermi energy for the $SiPd_3$ subcluster of Fig. 1(a) monolayer; (b) contour map of the composite Pd(d)-Si(p)antibonding/Si(p)-Si(p)bonding molecular-orbital wavefunction at the Fermi energy for the Pd_3Si_6 subcluster of Fig. 1(b) monolayer. The solid and dashed contours represent positive and negative values of the wavefunction, respectively.

Fig. 4. Subcluster local electronic density of states for an $MoSi_2$ monolayer, as computed by the partitioned scattered-wave method. The principal bonding, nonbonding, and antibonding characters of the component molecular orbitals are indicated.

Fig. 5. Contour maps of the $SiMo_3$ subcluster Mo(d)-Si(d) bonding molecular-orbital wavefunction at the Fermi energy of an $MoSi_2$ monolayer, plotted in (a) the monolayer plane and in (b) a plane perpendicular to the monolayer and containing two Mo atoms. Solid and dashed contours represent positive and negative values of the wavefunction, respectively.

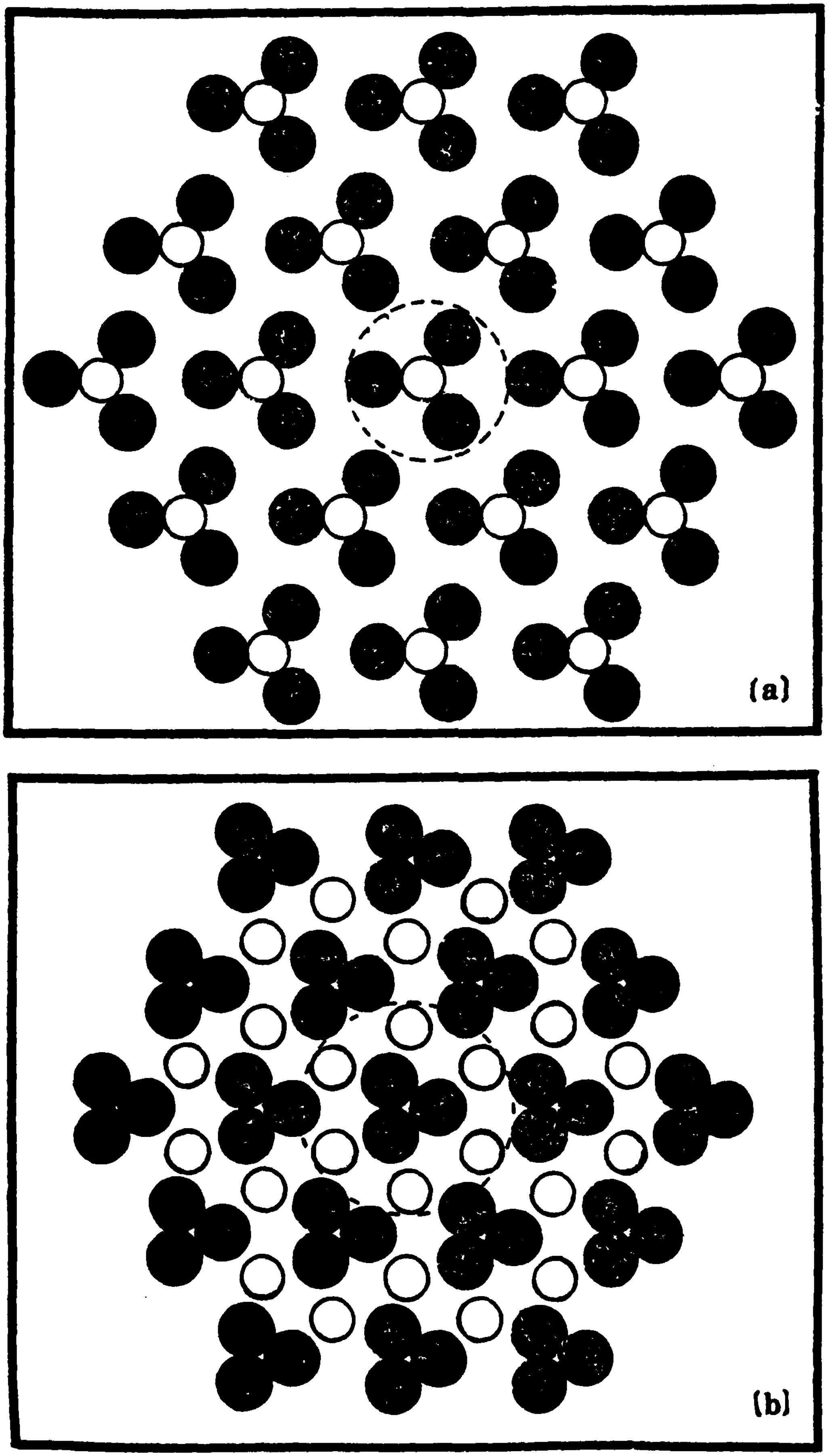

Fig. 1

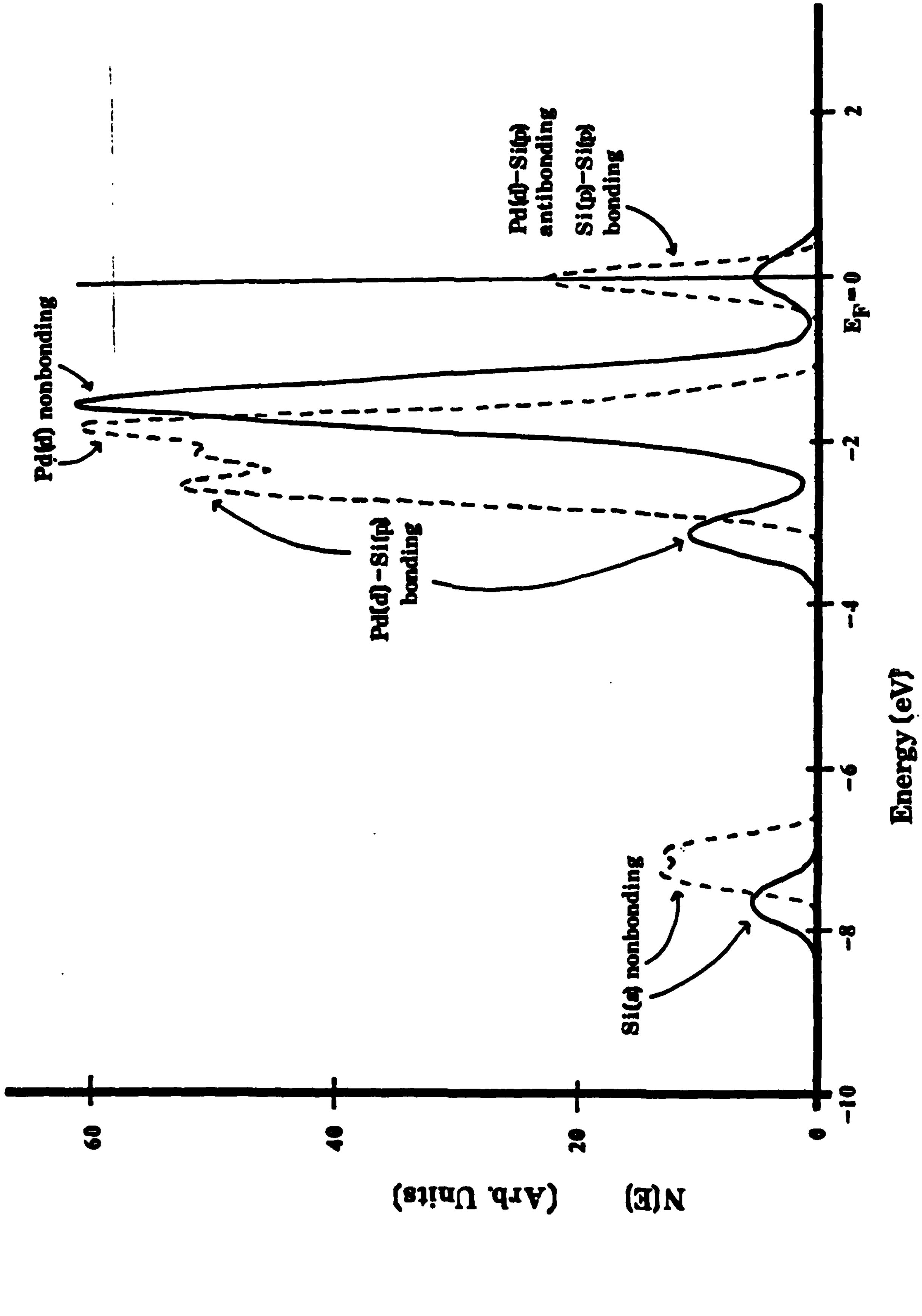

Pd(d) nonbonding
Pd(d)
Pd(d)-Si(p) bonding
Pd(d)-Si(p) antibonding
Si(p)-Si(p) bonding
Si(s) nonbonding
$E_F = 0$
Energy (eV)
N(E) (Arb. Units)
-10
-8
-6
-4
-2
0
2
0
20
40
60

Fig. 2

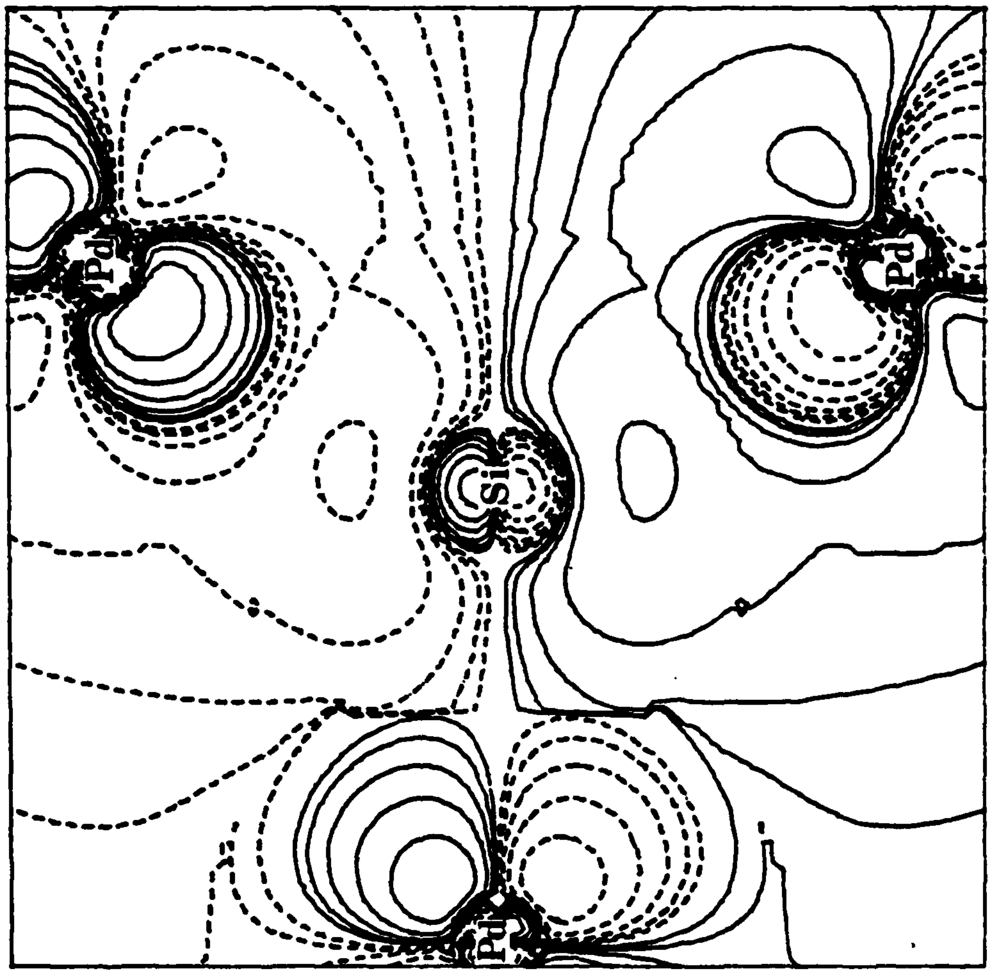

Fig. 3(a)

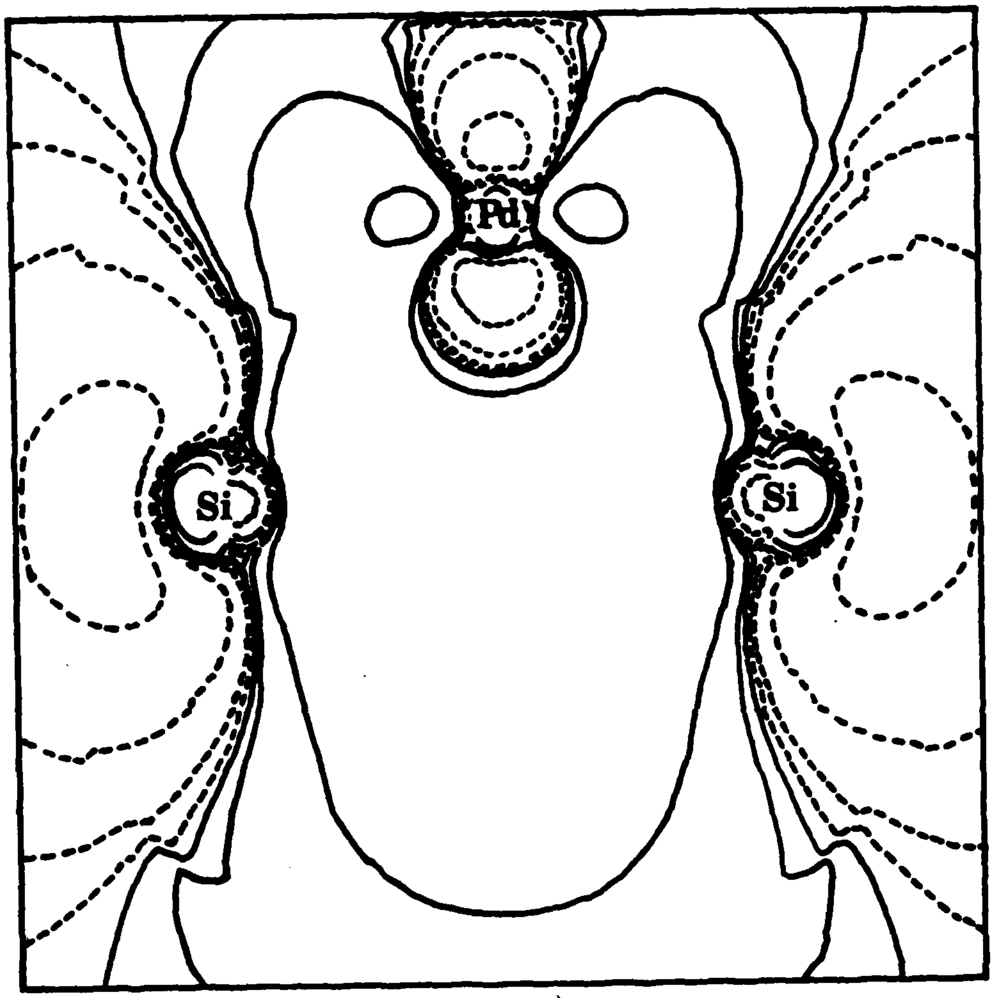

Fig. 3(b)

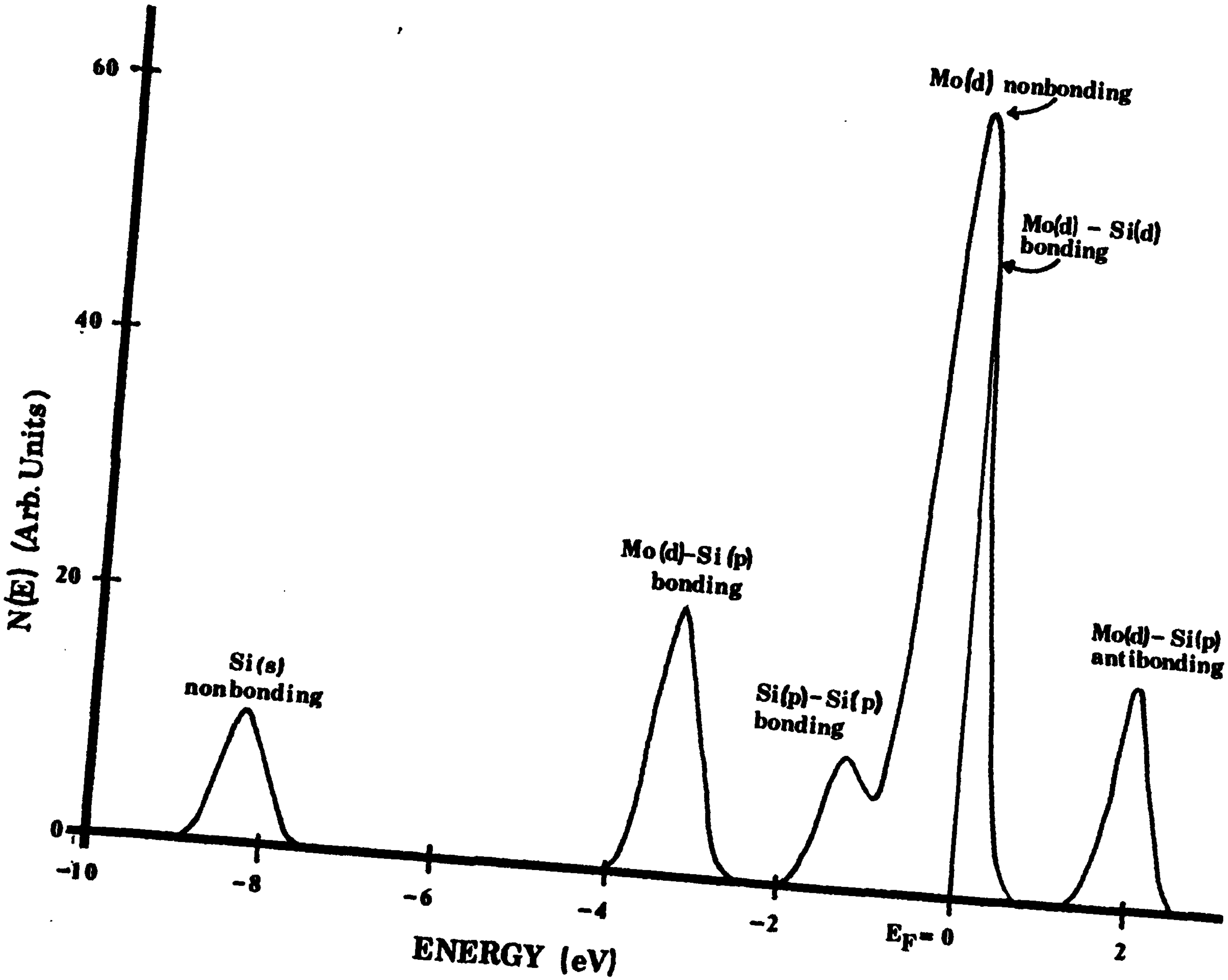
Mo(d) nonbonding
Mo(d) – Si(d) bonding
Mo(d)–Si(p) bonding
Si(p)–Si(p) bonding
Si(s) nonbonding
Mo(d)– Si(p) antibonding
N(E) (Arb. Units)
60
40
20
0
–10
–8
–6
–4
–2
$E_F = 0$
2
ENERGY (eV)

Fig. 4

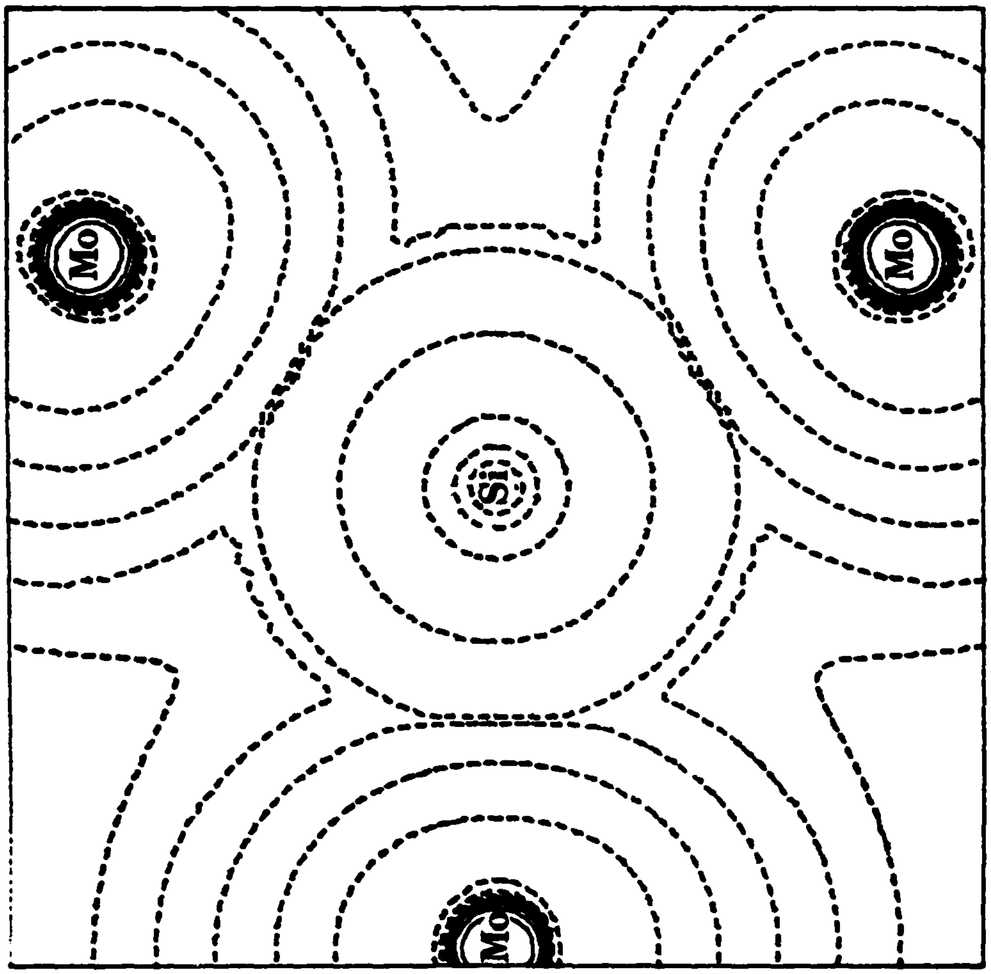

Fig. 5(a)

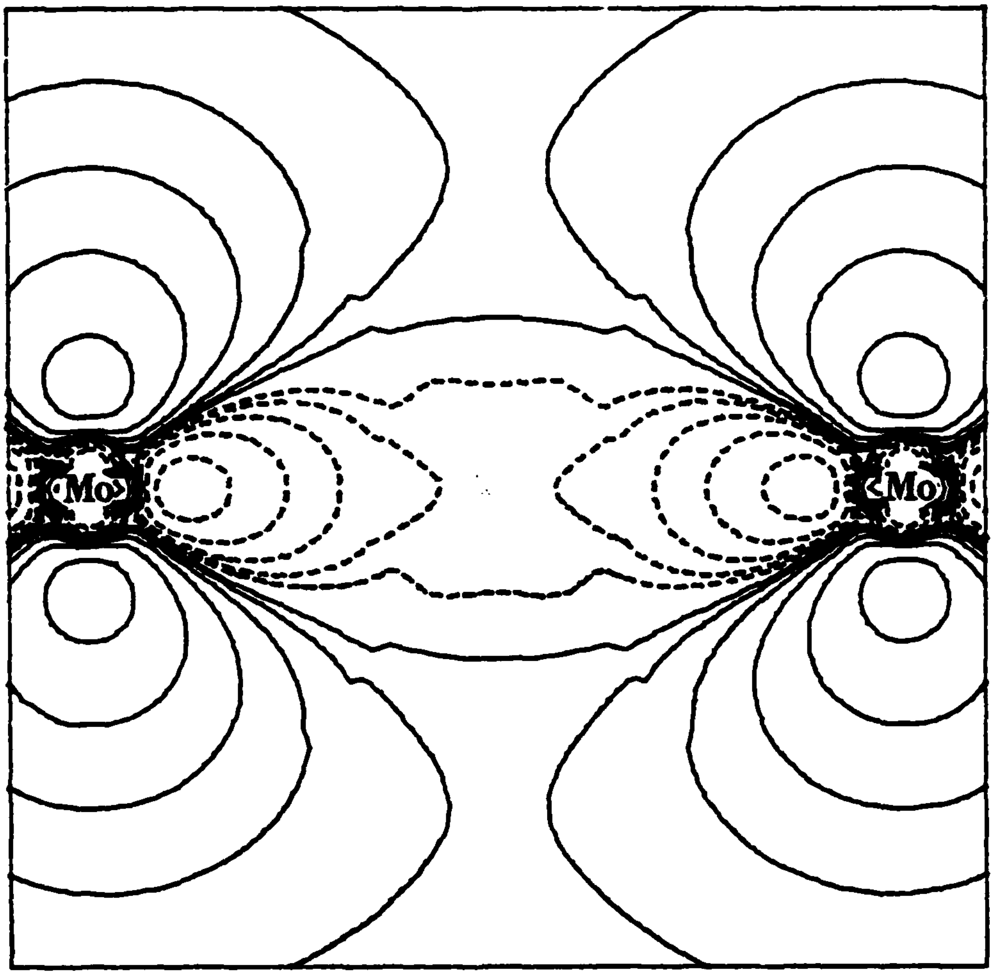

Fig. 5(b)

END

FILMED

12-84

DTIC